International Journal of Automation and Computing 1 (2004) 35-41

Simplified EKF Based Sensorless Direct Torque Control of Permanent Magnet Brushless AC Drives

Yong Liu*, Ziqiang Zhu, David Howe
Department of Electronic and Electrical Engineering, University of Sheffield, Mappin Street, Sheffield S1 3JD, UK

Abstract: A simplifed extended Kalman filter (EKF) based sensorless direct torque control technique for a permanent magnet brushless AC drive is proposed. Its performance is compared with that obtained with other sensorless methods for estimating the rotor speed and position from a stator flux-linkage. Since the EKF has an inherently adaptive filtering capability and does not introduce phase delay, the technique provides better speed estimates. In addition, the technique is easy to implement and requires minimal computation.

Keywords: Brushless motor, direct torque control (DTC), extended Kalman filter (EKF), permanent magnet, sensorless.

1 Introduction

Due to their high efficiency and excellent servo control performance, permanent magnet brushless ac (BLAC) motors are now used extensively. Of the various proposed control methods, direct torque control (DTC) is the most attractive one since it results in the best steady-state and dynamic performance. Originally developed for induction machine drives[1,2], DTC directly controls flux-linkage and electromagnetic torque, with due consideration for the electrical machine, power electronic inverter and control strategy at a system level, since a relationship is established directly between torque, flux and optimal inverter-switching to achieve a fast torque response. In addition to exhibiting a superior dynamic performance, it is less sensitive to parameter variations and simpler to implement than conventional scalar and vector control methods. Thus, the DTC strategy has also been applied to permanent magnet BLAC drives[3].

Numerous techniques have been proposed for sensorless DTC[4], the simplest, for BLAC motors, being based on either rotor or stator flux-linkage position estimates. Although rotor speed can be deduced directly from a rotor flux-linkage, it is preferable to derive rotor speed and stator flux-linkage position information from a stator flux observer, since while both stator flux and rotor flux rotate at synchronous speeds, the stator flux has to be observed in order to maintain electromagnetic torque at a demanded value[5]. However, when a flux observer is employed, a low-pass filter is required in order to extract rotor speed information[6], which introduces phase delay and may cause a control system to become unstable. Thus, the choice of filter parameters is a compromise between achieving good sensorless performance and minimizing phase delay. However, an extended Kalman filter (EKF) can be used as both state observer and filter, and, thereby, eliminate the phase delay problem. The sensorless DTC of a BLAC motor with an interior-magnet rotor topology was considered in [7]. However, it employed a full-order EKF state observer, and required relatively complex matrix calculations, which made it difficult to implement in practice, hence only simulated results were presented.

In this paper, the basic principle of DTC for BLAC drives is described and simulated, and experimental results are presented. A simplified EKF is combined with a stator flux observer to estimate the speed of a surface-mounted magnet motor and the position of a stator flux-linkage vector. It results in excellent dynamic performance and is easy to implement, making it potentially more attractive than previous approaches.

2 DTC control strategy

2.1 BLAC drive system

The specification for a BLAC motor is given in Table 1, and the main elements of a DSP-based drive system are shown in Fig.1. To enable a comparison with values obtained from sensorless techniques, an encoder is used to measure actual rotor position and deduce speed from the differential of position.

All control algorithms are implemented in a TMS-320C31DSP. The DAC board has four 12-bit digital-to-analogue converter (AD767) channels, which are used to output parameters such as motor speed and phase current. Its output port provides gate drive signals for inverter switching devices. Each ADC board has four 12-bit analogue-to-digital converter (AD678) channels

Manuscript received March 7, 2004; revised August 20, 2004

*Corresponding author. *E-mail address*: elp01yl@sheffield.ac.uk

and a 12-bit digital input parallel port. In addition, there are current transducers (LEM LA25-NP) and voltage transducers (LEM LV25-P). Phase currents and inverter DC link voltage are measured and sampled by the transducer board and ADC board, respectively. The encoder board is simply an interface between the DSP and the incremental encoder.

Table 1 Specification for a surface-mounted BLAC motor

DC link voltage (U)	70
Number of pole-pairs	1
Rated speed (rpm)	3000
Phase resistance (Ω)	0.466
Excitation flux-linkage (Wb)	0.0928
Winding inductance ($L_s = L - M$) (mH)	4.8
Rotor and load inertia (kgm^2)	8.0×10^{-4}
Damping factor (Nm/(rad/s))	1.0×10^{-4}

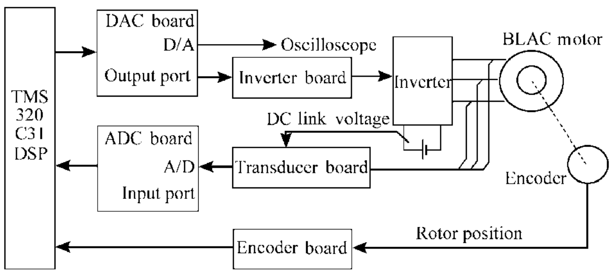

Fig.1 Schematic of a BLAC drive

2.2 DTC control strategy

In a stationary reference frame, a stator voltage equation is:

$$\bar{u} = R\bar{i} + \frac{d\bar{\psi}}{dt} \tag{1}$$

where R is the stator winding resistance and $\bar{\psi}$ is the stator flux-linkage vector, which can be derived from measured stator voltage $\bar{u}$ and current $\bar{i}$ as:

$$\bar{\psi} = \int (\bar{u} - R\bar{i})dt \tag{2}$$

Equation (2) can be expressed in a stationary α, β reference frame as:

$$\psi_\alpha = \int (u_\alpha - Ri_a)dt \tag{3}$$

$$\psi_\beta = \int (u_\beta - Ri_\beta)dt \tag{4}$$

The magnitude of stator flux-linkage can be obtained by:

$$\psi_s = \sqrt{\psi_\alpha^2 + \psi_\beta^2} \tag{5}$$

It should be noted that only stator resistance is required to be known in these equations. In a stationary reference frame, electromagnetic torque can be calculated by:

$$T = \frac{3}{2}p(\psi_\alpha i_\beta - \psi_\beta i_\alpha) \tag{6}$$

where p is the number of pole-pairs.

As can be seen from Table 2, stator voltage in a stationary reference frame can be obtained from the DC link voltage and the desired switching space vector, while stator current can be obtained from the 3-phase to 2-phase coordinate transformation.

$$\begin{bmatrix} i_\alpha \\ i_\beta \end{bmatrix} = \frac{2}{3}\begin{bmatrix} 1 & -\frac{1}{2} & -\frac{1}{2} \\ 0 & \frac{\sqrt{3}}{2} & -\frac{\sqrt{3}}{2} \end{bmatrix}\begin{bmatrix} i_a \\ i_b \\ i_c \end{bmatrix} \tag{7}$$

Table 2 Stator voltages in a stationary reference frame

	U_α	U_β
$V_1(100)$	$2U_{dc}/3$	0
$V_2(110)$	$U_{dc}/3$	$U_{dc}/\sqrt{3}$
$V_3(010)$	$-U_{dc}/3$	$U_{dc}/\sqrt{3}$
$V_4(011)$	$-2U_{dc}/3$	0
$V_5(001)$	$-U_{dc}/3$	$-U_{dc}/\sqrt{3}$
$V_6(101)$	$U_{dc}/3$	$-U_{dc}/\sqrt{3}$

Since in a symmetrical 3-phase winding with an isolated star-point, $i_a + i_b + i_c = 0$, the transformation can be simplified as:

$$i_\alpha = i_a \tag{8}$$

$$i_\beta = (i_a + 2i_b)/\sqrt{3} \tag{9}$$

Fig.2 shows the positions of the six voltage vectors in a stationary reference frame. The six sectors of the circular locus, which select the required voltage vector in terms of stator flux-linkage position, are also shown. Flux and torque commands are obtained by comparing the estimated electromagnetic torque and stator flux-linkage with demanded values. As can be seen from Table 3, the inverter's switching states can be determined according to the flux and torque commands from the outputs of two regulators, and the sector in which the stator flux-linkage is located. Fig.3 shows a block diagram of the direct torque controlled BLAC drive. The incremental encoder which provides speed feedback is subsequently replaced by an EKF based sensorless observer.

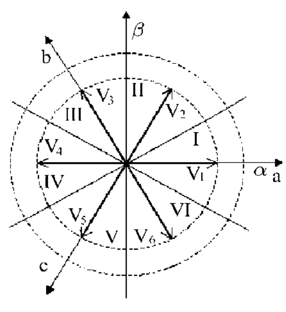

Fig.2 Voltage vectors

Table 3 A voltage space vector switching table

Flux		1		0	
Torque		1	0	1	0
Section	I	$V_2(110)$	$V_6(101)$	$V_3(010)$	$V_5(001)$
	II	$V_3(010)$	$V_1(100)$	$V_4(011)$	$V_6(101)$
	III	$V_4(011)$	$V_2(110)$	$V_5(001)$	$V_1(100)$
	IV	$V_5(001)$	$V_3(010)$	$V_6(101)$	$V_2(110)$
	V	$V_6(101)$	$V_4(011)$	$V_1(100)$	$V_3(010)$
	VI	$V_1(100)$	$V_5(001)$	$V_2(110)$	$V_4(011)$

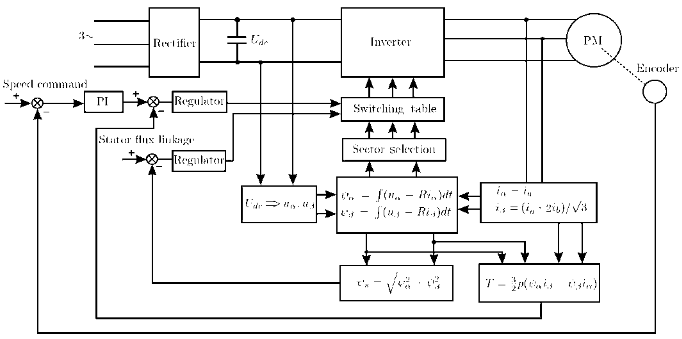

Fig.3 DTC of a BLAC drive

3 DTC drive with encoder

3.1 Simulation results

As shown in Fig.3, the implementation of DTC includes a stator flux observer, an electromagnetic torque estimator, a PI speed regulator, and an optimal switching table.

Using a MATLAB/SIMULINK based simulation model, the performance of the DTC system was simulated. Fig.4 shows the predicted variation of speed and electromagnetic torque of the BLAC motor in response to a step change in demanded speed from 1500 to 3000 rpm/s; while Fig.5 shows the steady-state phase current waveform and the locus of the stator flux-linkage at 3000rpm.

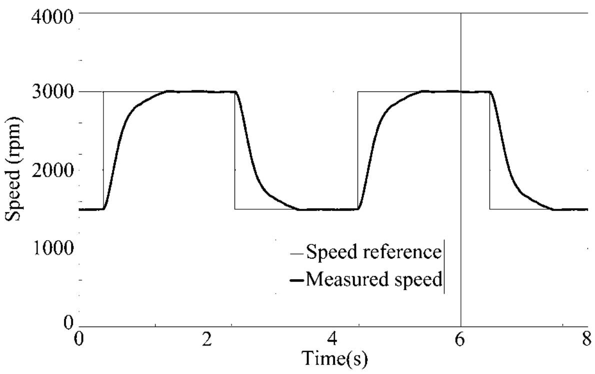

(a) Speed

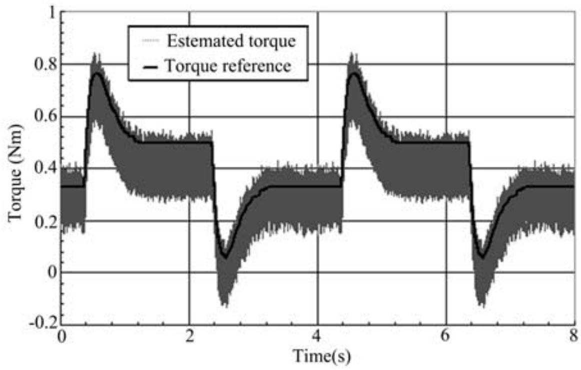

(b) Electromagnetic torque

Fig.4 Simulated speed and electromagnetic torque

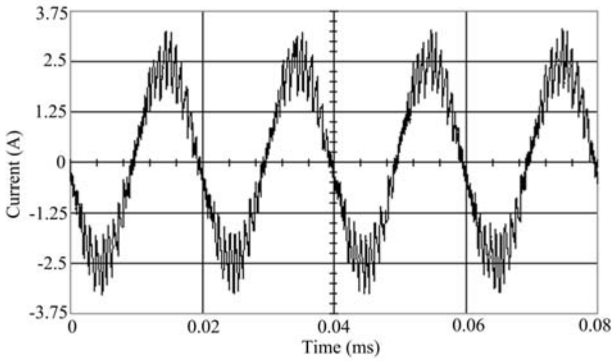

(a) Phase A current

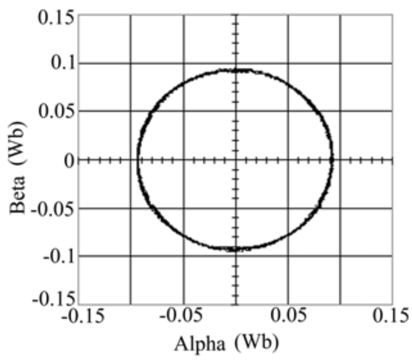

(b) The locus of the stator flux-linkage

Fig.5 Simulated phase current and stator flux linkage (speed=3000rpm)

3.2 Experimental results

The DTC algorithm was implemented on the TMS320C31 DSP with a sampling period fixed at $50\mu s$. Fig.6 shows measured speed and electromagnetic torque when commanded speed was changed from 1500 to 3000 rpm, while Fig.7 shows the steady-state phase current waveform and locus of the stator flux-linkage at 3000 rpm. As can be seen, good agreement is achieved between simulated and measured results.

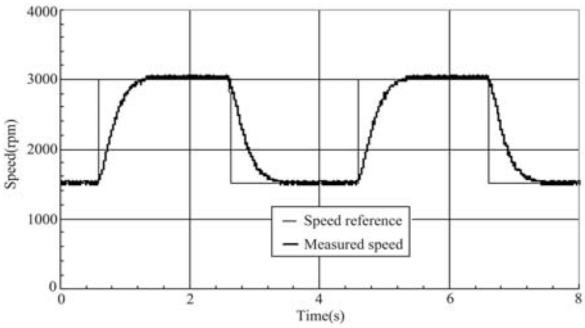

(a) Speed

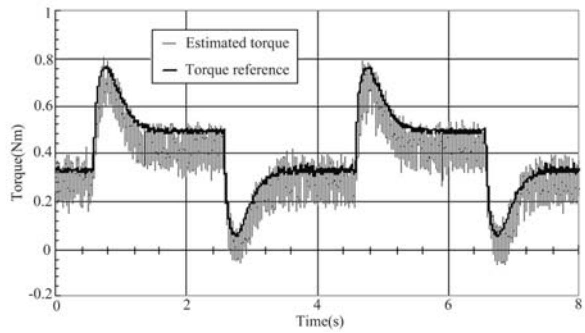

(b) Electromagnetic torque

Fig.6 Measured speed and electromagnetic torque

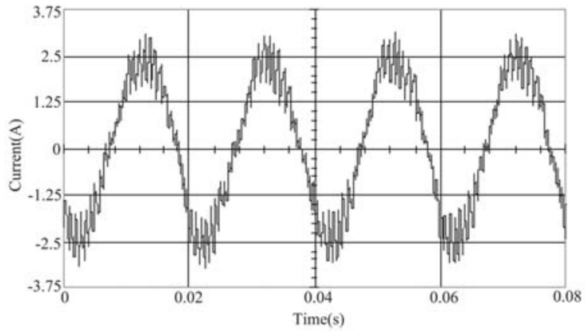

(a) Phase a current

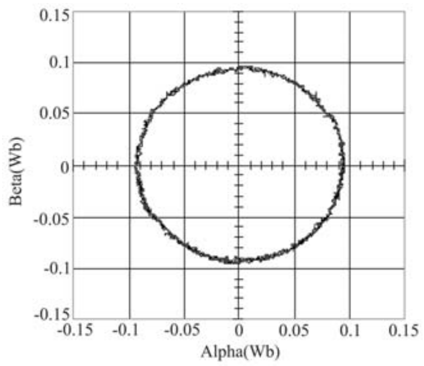

(b) The locus of the stator flux linkage

Fig.7 Measured phase current and stator flux linage (speed=3000rpm)

4 Sensorless direct torque control

4.1 Conventional approach

As mentioned earlier, since a stator flux-linkage is required in order to implement direct torque control, the estimation of rotor speed from a stator flux-linkage is common. After calculating equations (1)-(4), the angular position of the stator flux-linkage vector can be obtained as in [5]:

$$\theta_s = \arctan\frac{\psi_\beta}{\psi_\alpha} \tag{10}$$

Therefore, the rotational speed of the stator flux-linkage is given as:

$$\omega = \frac{d\theta_s}{dt} \approx \frac{\theta_{s(k)} - \theta_{s(k-1)}}{T_s} \tag{11}$$

where $\theta_{s(k)}$ and $\theta_{s(k-1)}$ represent the position of the stator flux-linkage vector at sample time t_k and t_{k-1} respectively and $T_s = (t_k - t_{k-1})$.

4.2 Simplified EKF approach

A discrete-time, non-linear dynamic system can be expressed in a state-space form as follows:

$$x(k+1) = f(x(k), k) + g(u(k), k) + w(k) \tag{12}$$

$$y(k) = h(x(k), k) + v(k) \tag{13}$$

where $u(k)$ and $y(k)$ are input and output signals respectively, and $w(k), v(k)$ are process noise and measurement noise respectively. $x(k)$ is the state vector which can be estimated by an EKF and is given by:

$$\hat{x}(k+1) = f(\hat{x}(k), k) + g(u(k), k) + K_k[y(k) - h(\hat{x}(k), k)] \tag{14}$$

Kalman gain K_k is determined using a Riccati difference equation (RDE)[7,8]. However, it requires very complex matrix calculations and therefore takes significant computing time.

In a DTC BLAC motor the output variables of the EKF may be chosen as:

$$\begin{bmatrix} y_1(k) \\ y_2(k) \end{bmatrix} = \begin{bmatrix} \psi_\beta \\ \psi_\alpha \end{bmatrix} \tag{15}$$

while the state variables are chosen as speed ω and position θ_s of a stator flux-linkage, and the double integration of noise w'. A speed identification model based on the EKF can then be established.

Since ψ_α and ψ_β, are the sine and cosine of the stator flux-linkage vector position (in order to simplify the model, in particular the computation of the Kalman gain), the output variables in (15) are expressed in normalized form as:

$$\begin{bmatrix} y_1(k) \\ y_2(k) \end{bmatrix} = \begin{bmatrix} \cos\theta_s(k) \\ \sin\theta_s(k) \end{bmatrix} + \begin{bmatrix} v_1(k) \\ v_2(k) \end{bmatrix} \tag{16}$$

Therefore, with a state vector $x = [\theta_s, \omega, w']^T$ and input $u(k) = 0$, the state-space model described in equations (12) and (13) can be written as:

$$x(k+1) = Fx(k) + w(k) \tag{17}$$

$$y(k) = h(x(k)) + v(k) \tag{18}$$

where $F = \begin{bmatrix} 1 & T_s & 0 \\ 0 & 1 & 1 \\ 0 & 0 & 1 \end{bmatrix}$, T_s is the sampling time and $h(x(k)) = \begin{bmatrix} \cos\theta_s(k) \\ \sin\theta_s(k) \end{bmatrix}$.

The Kalman filter gain can then be significantly simplified, and given as:

$$K = \begin{bmatrix} 0 & k_1 \\ 0 & k_2 \\ 0 & k_3 \end{bmatrix} \begin{bmatrix} \cos\hat{\theta}_s & \sin\hat{\theta}_s \\ -\sin\hat{\theta}_s & \cos\hat{\theta}_s \end{bmatrix} \tag{19}$$

where k_1, k_2, and k_3 are tuning parameters. They can be pre-computed from simulations, by using for example, the Matlab DLQE command for Kalman estimator design in discrete-time systems.

From the aforementioned, it can be shown that the rotor speed and position can be estimated using the following equations:

$$\varepsilon(k) = y_2(k)\cos\hat{\theta}_s(k) - y_1(k)\sin\hat{\theta}_s(k) \tag{20}$$

$$\hat{\theta}_s(k+1) = [\hat{\theta}_s(k) + T_s\hat{\omega}(k) + k_1\varepsilon(k)] \tag{21}$$

$$\hat{\omega}(k+1) = \hat{\omega}(k) + w'(k) + k_2\varepsilon(k) \tag{22}$$

$$w'(k+1) = w'(k) + k_3\varepsilon(k) \tag{23}$$

where $\hat{\theta}_s$ and $\hat{\omega}$ are estimated position and speed respectively.

It should be noted that the aforementioned is similar to that described in [8]. However, in [8], it is used to extract the rotor speed and position from the relatively noisy outputs of a resolver.

Fig.8 shows a block diagram of the simplified EKF which was used in the sensorless DTC system. The algorithm requires only six multiplications and two trigonometric operations and is easily implemented in a DSP.

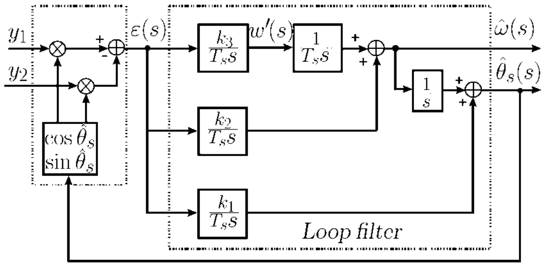

Fig.8 Block diagram of a simplified EKF

5 Comparison of estimated and measured rotor speed

Fig.9 compares measured and derived speed profiles when the demanded speed of the DTC BLAC motor varies between 1500 rpm and 3000 rpm. The speed feedback signal was obtained from the optical encoder or the estimated speed, both with and without a filter.

As shown in Fig.9 (a), when speed is estimated from the stator flux-linkage without a speed filter, it exhibits significant noise as a result of differentiating the estimated flux position. Therefore it cannot be used for speed feedback. While a flux filter may reduce noise, it has little effect on estimated speed[6]. Hence a speed filter is essential for speed control and a low pass filter is employed on the derived speed signal. However, as can be observed in Fig.9 (b), this results in significant phase lag. In contrast, when the EKF technique is employed, it results in estimated speed being noise-free with zero phase delay, as shown in Fig.9 (c).

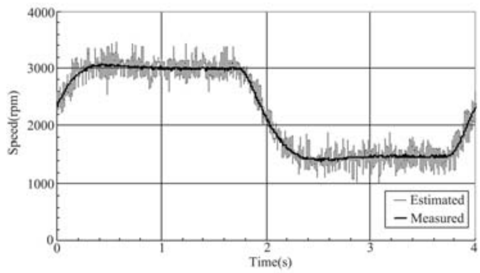

(a) Using an encoder for feedback, estimated speed derived from a stator flux-linkage without a speed filter

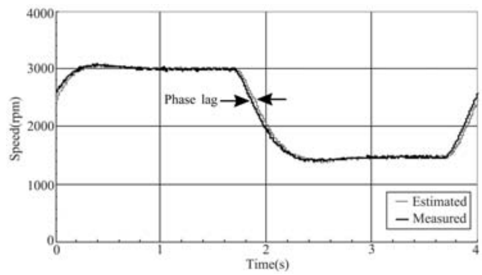

(b) Using estimated speed for feedback, speed derived from a stator flux-linkage with a speed filter

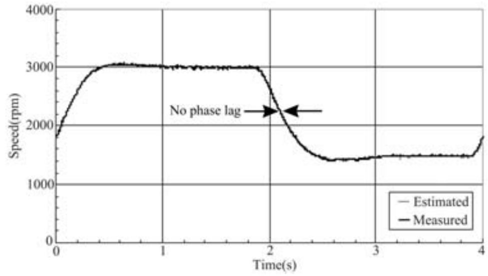

(c) Using estimated speed for feedback, speed derived from a stator flux-linkage by using a simplified EKF

Fig.9 Comparison of measured and estimated speed profiles

6 Comparison of estimated and measured rotor position

The DTC algorithm only needs information from a stator flux-linkage vector and does not require rotor position information. However, in order to compare estimated rotor position with that measured by an encoder, stator flux-linkage position is converted to rotor position by subtracting the load angle δ, which can be calculated using the electromagnetic torque equation:

$$T = \frac{3p\psi_s}{2L_s}\psi_r \sin(\delta) \tag{24}$$

in which torque is estimated from the flux observer and the measured current in equation (6).

Therefore load angle and rotor position can be calculated as:

$$\delta = \arcsin\left(\frac{2L_sT}{3p\psi_s\psi_r}\right) \tag{25}$$

and

$$\theta_r = \theta_s - \delta \tag{26}$$

By way of example, Fig.10 compares the accuracy of a rotor position derived from an estimated stator flux-linkage using equations (10) and (26), to that derived using the EKF technique and equations (21) and (26). As can be seen, error in estimated rotor position is much smaller when the EKF is employed.

7 Conclusions

A simplified EKF-based sensorless direct torque control technique has been presented. Compared to conventional techniques for estimating the position of a stator flux-linkage vector and the rotor speed directly from a stator flux-linkage, it is easier to implement and provide improved estimates of speed and position, since an EKF has an inherently adaptive filtering capability and, therefore does not introduce phase delay.

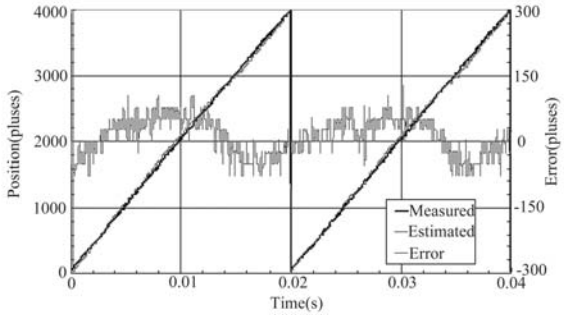

(a) Estimated directly from a stator flux-linkage

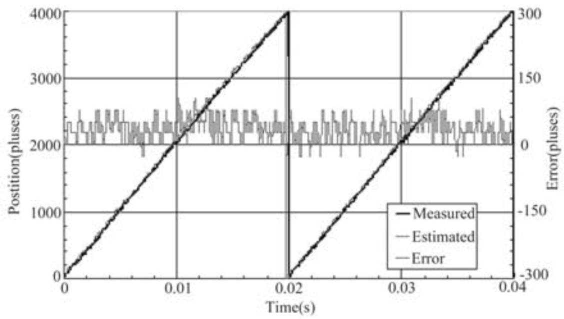

(b) Estimated by using an EKF

Fig.10 Comparison of measured and estimated rotor positions

References

[1] M. Depenbrock, Direct self-control of inverter-fed induction machine, *IEEE Trans. Power Electronics*, vol. 3, no. 4, pp. 420−429, Oct. 1988.

[2] I. Takahashi, T. Noguchi, A new quick-response and high-efficiency control Strategies of an induction motor, *IEEE Trans. Industry Applications*, vol. 22, no. 5, pp. 820−827, Sep./Oct. 1986.

[3] L. Zhong, M. F. Rahman, W. Y. Hu, K. W. Lim, Analysis of direct torque control in permanent magnet synchronous motor drives, *IEEE Trans. Power Electronics*, vol. 12, no. 3, pp. 528−536, May, 1997.

[4] M. Fu, L. Xu, A sensorless direct torque control technique for permanent magnet synchronous motors, *Conference Record of the 1999 IEEE Thirty-Fourth IAS Annual Meeting*, Industry Applications Conference, vol. 1, pp. 159−164, 1999.

[5] P. Vas, *Sensorless Vector and Direct Torque Control*, Oxford University Press, 1998.

[6] J. X. Shen, Z. Q. Zhu, D. Howe, Improved speed estimation in sensorless PM brushless AC drives, *IEEE Transactions on Industry Applications*, vol. 38, no. 4, pp. 1072−1080, 2002.

[7] V. Comnac, M. N. Cirstea, F. Moldoveanu, D. N. Ilea, R. M. Cernat, Sensorless speed and direct torque control of interior permanent magnet synchronous machine based on extended Kalman-filter, *Proceedings of 2002 IEEE International Symposium on Industrial Electronics*, vol. 4, pp. 1142−1147, 2002.

[8] L. Harnefors, Speed estimation from noisy resolver signals, *Proc. Sixth International Conference on Power Electronics and Variable Speed Drives*, pp. 279−282, 1996.

Yong Liu received the B.Eng and M.Sc. degrees in electrical engineering from Zhejiang University, Hangzhou, China, in 1999 and 2002, respectively.

Since 2002, he has been with the Department of Electronic and Electrical Engineering, the University of Sheffield, Sheffield, U.K., where he is currently a PhD student. His research interests include control of electrical drives, in particular, the direct torque control of permanent magnetic brushless motors.

Ziqiang Zhu received the B.Eng. and M.Sc. degrees from Zhejiang University, Hangzhou, China, in 1982 and 1984, respectively, and was awarded the Ph.D. by the University of Sheffield, Sheffield, UK, in 1991, all in electrical and electronic engineering.

From 1984 to 1988 he lectured in the Department of Electrical Engineering at Zhejiang University. Since 1988, he has been with the University of Sheffield, where he is currently Professor of Electronic and Electrical Engineering. His current major research interests include applications, control, and design of permanent magnet machines and drives.

David Howe received the B.Tech and M.Sc. degrees from the University of Bradford, in 1966 and 1967, respectively, and a Ph.D. from the University of Southampton in 1974, all in electrical power engineering.

He has held academic posts at Brunel and Southampton Universities, and spent a period in industry with NEI Parsons Ltd working on electromagnetic problems related to turbo-generators. He is currently Professor of Electrical Engineering at the University of Sheffield, where he heads the Electrical Machines and Drives Research Group. His research activities span all facets of controlled electrical drive systems, with particular emphasis on permanent magnet excited machines. Prof. Howe is a Fellow of the Royal Academy of Engineering and a Fellow of the IEE, UK.